Korean J. Chem. Eng., **21**(1), 230-235 (2004)

Density Correlation of Solubility of C. I. Disperse Orange 30 Dye in Supercritical Carbon Dioxide

Jong-Kook Baek, Sunwook Kim*, Gwang-Soo Lee and Jae-Jin Shim†**

School of Chemical Engineering and Technology, Yeungnam University,
214-1 Dae-dong, Gyeongsan City, Gyeongbuk 712-749, Korea
*School of Chemical and Biochemical Engineering, University of Ulsan,
San 29, Moogeo-2-dong, Nam-gu, Ulsan 680-749, Korea
**Samill Industries, Ltd., Zone 2 of Seongseo Industrial Complex 2,
Daecheon-dong, Dalseo-gu, Daegu 704-329, Korea
(*Received 28 July 2003 • accepted 21 October 2003*)

Abstract−The solubility of C. I. Disperse Orange 30 (O30) dye in CO_2 has been measured by using a closed-loop (batch) solid-fluid equilibrium apparatus at temperatures between 313 and 393 K and at pressures between 11 and 33 MPa. Kumar and Johnston's equation based on Chrastil's concept has been used to describe the experimental solubility data. The solubility versus density plot appears much simpler than the solubility versus pressure plot. The isotherms are nearly straight and parallel to each other, as seen in the previous studies. Peng-Robinson equation of state (PR EOS) has also been used successfully in modeling the dye solubility in supercritical carbon dioxide as a function of pressure or density of the fluid phase. The validity of this method has been verified by the vapor pressure calculation.

Key words: Solubility, Disperse Dye, Supercritical Carbon Dioxide, Peng-Robinson Equation of State

INTRODUCTION

The conventional wet-dyeing industry, which discharges considerable amounts of wastewater containing highly concentrated, very little biodegradable surfactants, has been continuously raising pollution problems worldwide. Among the several researches aiming to replace the conventional process, supercritical fluid dyeing (SFD) has been particularly drawing attention: it is environmentally friendly because it does not require any surfactant nor dispersing agent [Saus et al., 1993; Chang et al., 1996]. Furthermore, energy consumption may be only a half that of the conventional dyeing process as the drying step is not necessary in the SFD process.

To develop and design this new process, a large amount of basic dye solubility data is necessary. Dye solubility in supercritical fluids (SCFs) has been measured [Haarhaus et al., 1995; Swidersky et al., 1996; Oezcan et al., 1997; Kautz et al., 1998; Tuma and Schneider, 1998; Muthukumaran et al., 1999; Sung and Shim, 1999]. Although there has been much research on solid solubility in SCF, the fluid-phase behavior of solids with very high molecular weights has not been fully understood yet. Some empirical equations have been used to correlate the solubility of large molecular-weight solids with pressure or density of the fluid. Chrastil [1982] derived a simple equation from equilibrium that shows the logarithm of solubility is proportional to the logarithm of fluid density. Fat'hi et al. [1998] and Oezcan et al. [1997] proved his theory is applicable to disperse dyes and anthraquinone derivatives. Kumar and Johnston [1988] derived a relationship between the solubility of solids in SCFs with the density or with the logarithm of density based on the approximate linearity of the slopes of the solubility isotherms in semi-log and log-log density plots. Bartle et al. [1992] correlated the solubility isotherms with PR EOS using the binary interaction parameters as an adjustable variable.

In this work the solubility of the O30 disperse dye in supercritical carbon dioxide was measured over a wide range of pressures and temperatures. The experimental data were correlated with Kumar and Johnston's two simple semi-empirical equations. The behavior of the solubility isotherms was analyzed and discussed. The experimental solubility data of disperse dyes in pure supercritical CO_2 was correlated with PR EOS by using the energy parameter obtained by correlation of the experimental data.

EXPERIMENTAL SECTION

1. Materials

The pure C. I. Disperse Orange 30 dye (Fig. 1) with molecular weight of 450 g/mol that contains neither dispersing agents nor surfactants was obtained from LG Chemical. Its melting point, 398.56 K, and the heat of fusion, 17.08 kJ/mol, were measured by a differential scanning calorimeter. Its solid molar volume, 273 mL/mol, was measured by the volumetric method using helium that is close

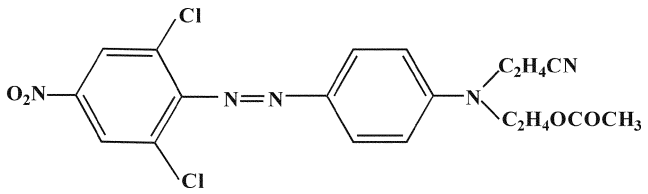

Fig. 1. The molecular structure of C. I. Disperse Orange 30 dye.

†To whom correspondence should be addressed.
E-mail: jjshim@yu.ac.kr
‡This paper is dedicated to Professor Hyun-Ku Rhee on the occasion of his retirement from Seoul National University.

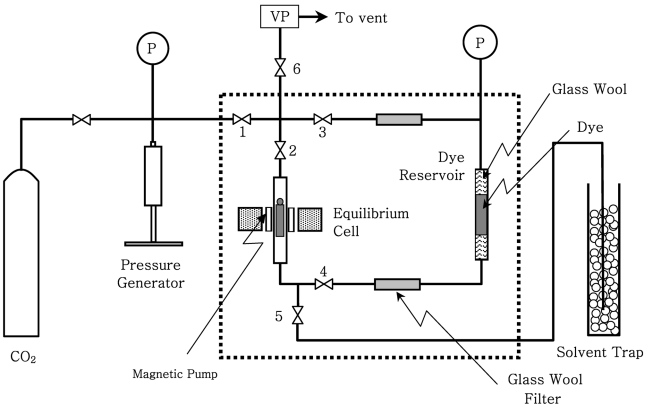

Fig. 2. Schematic diagram of the dye-solubility apparatus.

to an ideal gas [Baek, 2001]. CO_2 with purity of 99% was obtained from Daedong Oxygen. These materials were used without further purification.

2. Experimental Equipment

A closed-loop (batch) solid-fluid equilibrium apparatus was installed in a constant-temperature air bath that was controlled within ±1 K (Fig. 2). A high-pressure magnetic pump that consists of a piston, a cylinder and a magnetic coil was used to circulate the dye mixture along the loop by moving the piston up and down continuously. A small amount of dye was placed in the dye reservoir with both ends plugged with glass wool to prevent the dye powder from being entrained to the equilibrium cell. Two additional filters packed with glass wool were placed on both sides of the dye reservoir to block any traces of dye-powder entraining. These filters were cleaned after each series of measurements. A pressure transducer (Sensotec, Model TJE) and a signal indicator (Sensotec, Model GM) were installed and calibrated to read the pressure to ±0.01 MPa.

3. Experimental Procedure

Liquid CO_2 was pumped with a high-pressure metering pump (LDC/Milton Roy) into the system to make the desired pressure.

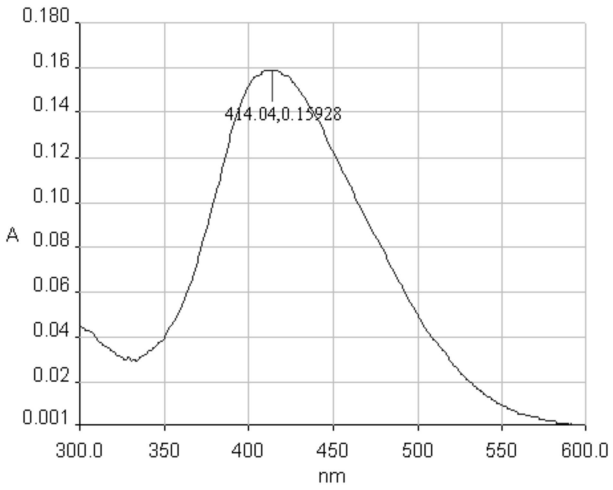

Fig. 3. The UV-Visible absorption spectrum for O30 dye in ethanol. A=log (I_0/I), where A is light absorbency, I_0 is the intensity of the incident light and I is the intensity of the transmitted light.

CO_2 placed in the isolated equilibrium system was circulated with the magnetic pump for 120 minutes until the equilibrium in dye solubility was reached. Then, the mixture in the equilibrium cell was slowly released to a trap filled with ethanol to collect the dissolved dye that remained in the cell. Some of the dye powder that was precipitated on the wall of the equilibrium cell during the depressurization step was recovered by washing with ethanol. These two dye-ethanol solutions were mixed and analyzed to figure out the dye content by using a UV/Visible spectrometer (Perkin-Elmer, Model Lambda 40). The maximum peak for the dye solution appeared at a wavelength of 414.0 nm (Fig. 3). The dye concentration in the equilibrium cell was calculated from the amount of CO_2 in the cell. To minimize the experimental uncertainty in the subsequent measurements, the ethanol remaining in the cell was completely removed by flushing with air, followed by being dissolved out with supercritical CO_2 four or five times. The equilibrium solubilities at different temperatures and pressures were also measured by the same way. The uncertainty in the dye solubility data is within ±5%.

THEORETICAL CONSIDERATIONS

1. Chrastil's Linear Density Correlation

Since Chrastil [1982] showed linear behavior of solubility with density in the early 1980's, there have been many studies showing that the logarithm of solubility of solid solutes in SCF is linearly proportional to the density or to the logarithm of density [Kumar and Johnston, 1988; Bartle et al., 1991; Oezcan et al., 1997; Sung and Shim, 1999]. Kumar and Johnston analyzed the linear behavior of solubility using the partial molar volume of solute that was evaluated with PR EOS. Based on this relationship, Sung and Shim [1999] modified Chrastil's and Kumar and Johnston's equations to correlate the experimental solubility data with density as follows:

$$\ln y_A = a + b/T + c\rho \tag{1}$$

$$\ln y_A = a' + b'/T + (c' + d'/T)\ln\rho \tag{2}$$

where y_A is the solubility of solid solute A, ρ is the fluid density, T is temperature, and a, b, c, a', b', c', and d' are the constants.

2. Density Correlation with Peng-Robinson Equation of State

To describe the effect of density on solubility, an equation for gas-solid equilibrium may be employed, assuming that the fluid is in the extended gas state:

$$y_A \phi_A P = P_A^v \exp\left(\frac{v_A^s P}{RT}\right) \tag{3}$$

where y_A is the solubility of solute A, ϕ_A is the fugacity coefficient of A, P_A^v is the vapor pressure of A, and v_A^s is the solid molar volume of A. The fugacity coefficient of A is related to the volume and pressure as follows [Prausnitz et al., 1999]:

$$RT\ln\phi_A = \int_v^\infty \left[\left(\frac{\partial P}{\partial n_A}\right)_{T,V,n_B} - \frac{RT}{V}\right] dV - RT\ln Z \tag{4}$$

where V is the volume of the mixture, n_A is the number of moles of solute A, n_B is the number of moles of fluid solvent B, and Z (=PV/RT) is the compressibility factor of the mixture. The first term in the integral, $(\partial P/\partial n_A)_{T,P,n_B}$, may be replaced by $\bar{v}_A/\kappa V$, where $\bar{v}_A$ is the partial molar volume of solute A and κ is the compressibility

factor of the fluid [Modell and Reid, 1983].

The relationship between solubility and density cannot be directly derived from Eqs. (3) and (4). Therefore, Kumar and Johnston [1988] defined a new fugacity coefficient of i, ψ_i, based on the density of the fluid:

$$\psi_i \equiv \phi_i Z \tag{5}$$

Using this equation, they reduced Eq. (4) to the following equation for a solid solute.

$$\ln \psi_A = \int_0^\rho \left[\frac{\overline{v}_A}{\kappa RT} - 1 \right] d\ln\rho \tag{6}$$

Also, the exponent on the right-hand side of Eq. (3) may be written as:

$$\frac{v_A^s P}{RT} = \int_0^P \left(\frac{v_A^s}{RT} \right) dP = \int_0^\rho \frac{v_A^s}{\kappa RT} d\ln\rho \tag{7}$$

Using the definition of ψ_i in Eq. (5) and the expression in Eq. (7), we can exclude pressure from the phase equilibrium relation in Eq. (3), transforming it into a density-dependent equation as follows:

$$\rho RT y_A \psi_A = P_A^v \exp \int_0^\rho \frac{v_A^s}{\kappa RT} d\ln\rho \tag{8}$$

Taking logarithms on both sides of Eq. (8), followed by rearranging the equation for the fluid phase mole fraction using Eq. (6) yields

$$\ln y_A = \ln\left(\frac{P_A^v}{RT} \right) + \int_0^\rho \frac{v_A^s - \overline{v}_A}{\kappa RT} d\ln\rho - \ln\rho_0 \tag{9}$$

where ρ_0 is the density at zero pressure. As the solubility near the zero density has not been defined yet, we cannot use Eq. (9) to calculate the solubility. Instead, the slope of the solubility isotherm (a in Eq. (1)) in a medium density SCF may be derived from Eq. (9) [Sung, 1998].

$$\left(\frac{\partial \ln y_A}{\partial \ln\rho} \right)_T = \frac{v_A^s - \overline{v}_A}{\kappa RT} \tag{10}$$

Since $\ln y_A$ is usually a linear function of $\ln\rho$, the slope of the solubility isotherm in the log-log plot is a positive constant. Therefore, the left-hand side of Eq. (10) must be a constant in the approximate density range of $0.5 \le \rho_r \le 2.0$ [Kumar and Johnston, 1988], where ρ_r is the reduced density. Outside of this range, either to zero density or to a very large density, the slope decreases to zero, forming a maximum solubility, and then further decreases to a very large negative value. Eq. (10) shows a similar shape as Kurnik and Reid's equation for the slope of the logarithm of solubility vs. pressure at constant temperature. Kurnik and Reid [1981] claimed that the solubility minimum or maximum exists when the partial molar volume is the same as the solid molar volume. We may expect a similar behavior of the dye solubility with density.

Using the partial molar volume of solute obtained from PR EOS [Sung, 1998], Eq. (10) may be expressed as follows:

$$\left(\frac{\partial \ln y_A}{\partial \ln\rho} \right)_T = \frac{v_A^s}{RTK_T} - \frac{v}{v-b} - \left[\frac{v}{(v-b)^2} + \frac{2v(\alpha a)(v-b)}{RT(v^2+2bv-b^2)^2} \right] b_A + \frac{2v(\alpha a)^{0.5}}{RT(v^2+2bv-b^2)} (\alpha_A a_A)^{0.5} (1-k_{AB}) \tag{11}$$

In the above equation we have two parameters: an energy parameter, a_A, and a size parameter, b_A. The fugacity coefficient of solute in SCF is then evaluated by the following equation that was derived from PR EOS [1976].

$$\ln \psi_A = \frac{b_A}{b}\left(\frac{Pv}{RT} - 1 \right) + \ln \frac{v}{v-b} - \frac{\alpha a}{2\sqrt{2}bRT} \left[\frac{2\sum_i y_i a_{Ai} \alpha_{Ai}}{a\alpha} - \frac{b_A}{b} \right] \ln \frac{v + (1+\sqrt{2}b)}{v + (1-\sqrt{2}b)} \tag{12}$$

The fugacity coefficient in Eq. (12) may be substituted into Eq. (3) to calculate the solubility of solids in supercritical fluids.

RESULTS AND DISCUSSION

1. Linear Solubility Isotherms using Chrastil's Density Correlation

The experimental solubility data for O30 dye are shown in Table 1. When they are plotted versus pressure at constant temperature, the solubility isotherms look complex as they cross each other near 15 MPa (Fig. 4). The same behavior was seen in previous studies on high molecular weight solid solutes [Swidersky et al., 1996; Sung, 1998; Tuma and Schneider, 1998]. It is difficult to analyze this kind of pressure behavior of solubility with a simple equation. When we plot them versus fluid density, however, we can see much sim-

Table 1. Experimental solubility data for C. I. Disperse Orange 30

Pressure (MPa)	Density (gmol/L)	Solubility ($y \times 10^6$)	Pressure (MPa)	Density (gmol/L)	Solubility ($y \times 10^6$)
	313.15 K			333.15 K	
11.46	15.94	8.01	13.57	12.28	9.51
13.28	17.03	9.57	15.27	13.96	11.40
17.27	18.45	12.24	15.80	14.35	11.68
20.61	19.23	14.59	17.85	15.55	15.38
22.73	19.63	17.58	18.44	16.00	16.45
27.02	20.30	21.56	20.12	16.50	19.02
29.40	20.62	23.44	23.70	17.57	26.12
30.80	20.79	25.90	25.09	17.91	30.01
31.09	20.83	26.05	27.45	18.41	34.06
			27.72	18.46	35.11
			29.51	18.79	39.11
			31.20	19.07	42.25
	363.15 K			393.15 K	
13.03	6.82	9.09	11.28	4.42	9.56
14.58	8.10	11.20	13.68	5.66	13.85
15.95	9.23	13.34	16.15	7.02	17.45
16.03	9.30	14.02	16.69	7.32	19.32
18.03	10.84	17.54	17.13	7.56	20.50
19.06	11.55	20.34	21.28	9.78	30.01
21.23	12.81	23.81	24.25	11.18	39.56
22.61	13.48	28.89	26.20	11.98	50.48
26.64	14.97	38.98	28.13	12.69	62.74
28.56	15.60	45.20	30.25	13.38	72.56
29.05	15.74	49.78	32.57	14.05	84.32
31.08	16.25	53.63			
32.10	16.49	58.03			

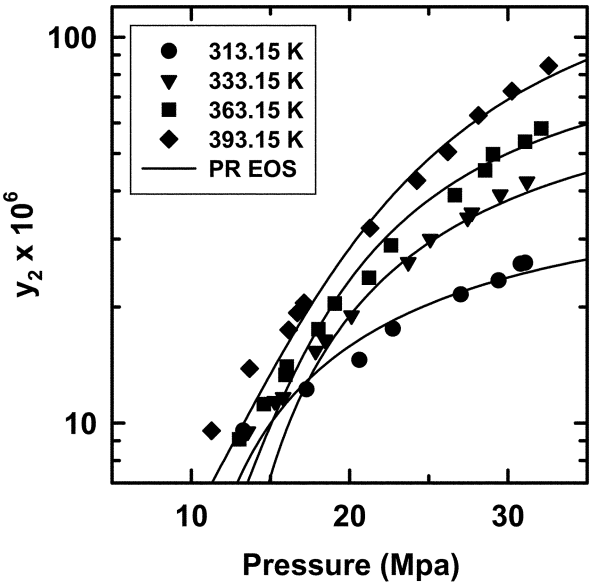

Fig. 4. The solubility of O30 dye in supercritical carbon dioxide as a function of pressure.

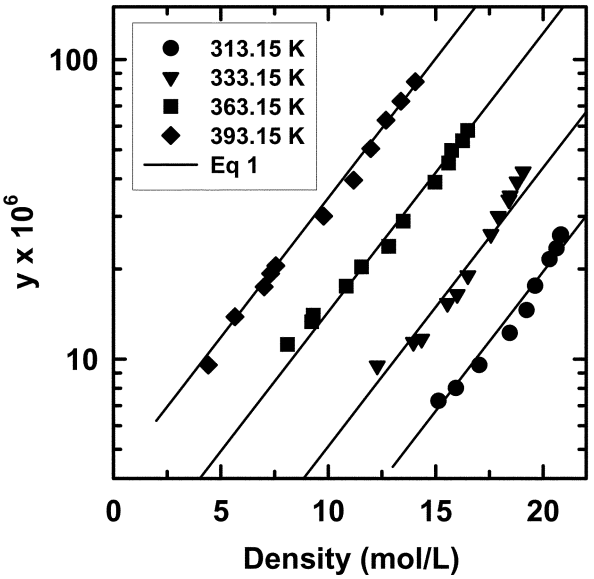

Fig. 5. The solubility of O30 dye in supercritical carbon dioxide with density.

pler near-straight lines, which are parallel to each other (Fig. 5). Both the density plot and the logarithm of density plot of the logarithm of the experimental solubility data are well described by Eqs. (1) and (2), respectively, though the latter is not shown here. The slopes in the log-log plot are shown in Table 2. The constants in Eqs. (1) and (2) were obtained from the lines that best describe the experimental data. The values of constants a, b, and c in Eq. (1) were 12.00, −4165, and 0.2141, respectively. And the values of constants a', b', c', and d' in Eq. (2) were 33.96, −1326, −17.02, and 8139, respectively. We observed a similar behavior for C. I. Disperse Blue 60 and C. I. Disperse Red 60 dyes in our previous study [Sung and Shim, 1999] where the logarithm of solubility in pure supercritical CO_2 was a linear function of either density or logarithm of density.

2. Solubility from the Density Correlation with Peng-Robinson Equation of State

PR EOS [1976] was used to correlate the solubility of O30 (Fig. 4). The size parameter for solute b_A, which is often called van der Waals size parameter, is taken as the close-packed volume of the solid molecule and is normally estimated from its critical volume. Unfortunately, the critical properties for very high molecular weight substances such as disperse dyes are usually unavailable and thus it is impossible for us to get their size parameters. Therefore, we assumed that b_A is nearly the same as the molar volume of the solid, v_A^s, which was measured experimentally in this research.

The temperature-dependent energy parameter for solid, $\alpha_A a_A$, is normally estimated from its critical properties. But, again, for high molecular weight solid, the critical properties are not known. It is very difficult to get the energy parameter value. One way is to use the solubility parameter of the binary mixture [Bartle, 1992]. The other way is to correlate the experimental solubility data. We chose the second method as the solubility parameter is not known either. Therefore, we first selected slopes of all the isotherms in the plot lny vs. lnρ that fit the data best with straight lines within the experimental density range. From the experimental solubility in CO_2, we estimated the attractive energy term $(\alpha_A a_A)^{0.5}(1-k_{AB})$ in Eq. (11). The results are shown in Table 2. These values for all the isotherms were then averaged to get a single value for this energy term, 3.22×10^{-6}, which can best describe the entire experimental solubility data

Table 2. Slopes of the log-log plots, the energy parameter and the vapor pressure of O30 dye

T (K)	Slope	$(\alpha_2 a_2)^{0.5}(1-k_{12})\times10^{-6}$	Vapor pressure (Pa)
313.15	4.08	3.75	2.646×10^{-4}
333.15	3.12	3.44	3.637×10^{-3}
363.15	2.00	2.79	0.159
393.15	1.89	2.88	3.313

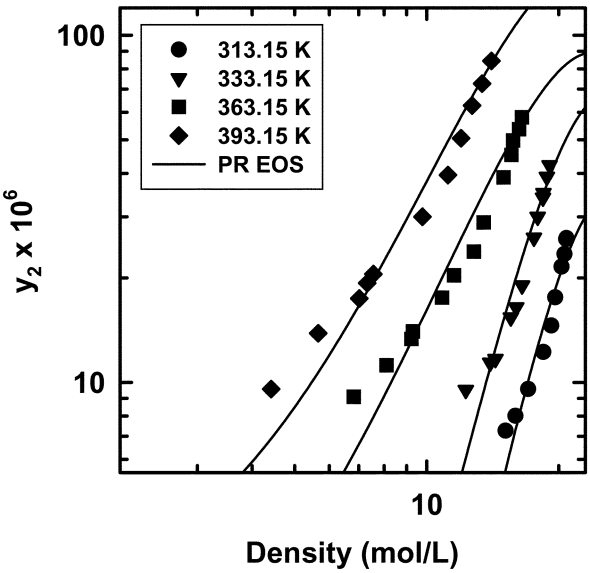

Fig. 6. The solubility of O30 dye in supercritical carbon dioxide as a function of density.

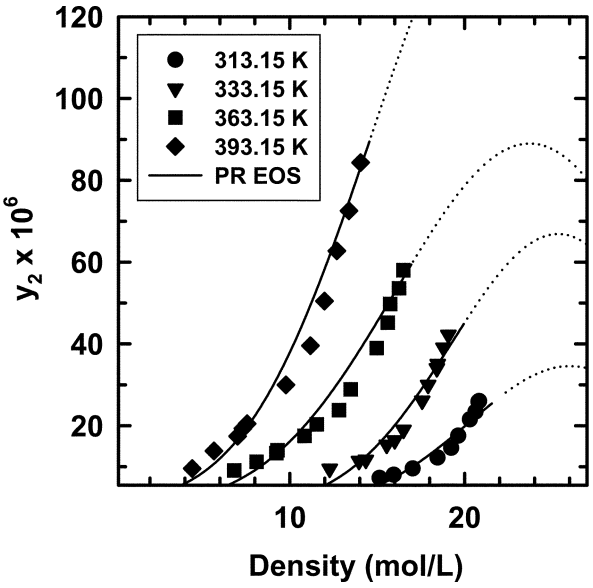

Fig. 7. The solubility of O30 dye in supercritical carbon dioxide as a function of density.

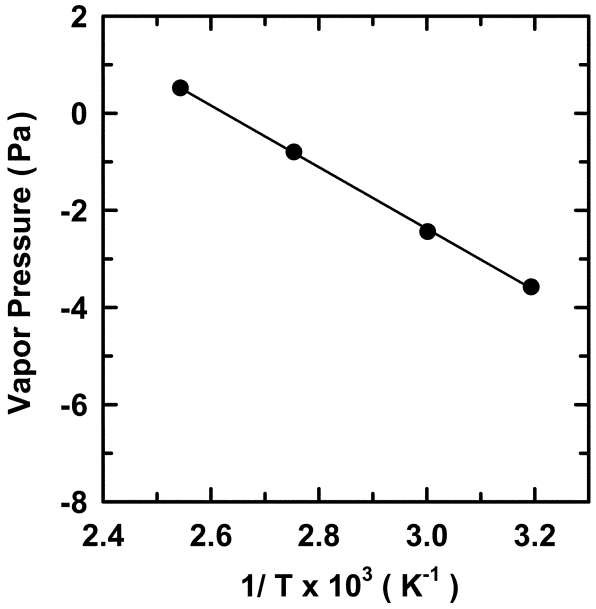

Fig. 8. Variation in the vapor pressure of O30 disperse dye with temperature.

for a given dyestuff. Once this energy term is obtained, the fugacity coefficient of the solute in SCF can be evaluated by Eq. (12). For the calculation of the mixture parameters, van der Waals one-fluid mixing rules, $a\alpha = \sum\sum x_i x_j (a\alpha)_{ij}$ and $b = \sum\sum x_i x_j b_{ij}$, were then employed. The cross parameters were obtained from the usual combining rules, $(a\alpha)_{ij} = \sqrt{(a\alpha)_{ii}(a\alpha)_{jj}}(1-k_{ij})$ and $b_{ij} = 1/2(b_i + b_j)$.

Using the size parameter and the energy parameter determined above, the solubility of O30 was calculated and is shown versus pressure (Fig. 4) and density (Fig. 6). The calculated isotherms fit the experimental data fairly well. When the solubility correlated with Peng-Robinson EOS in the limited density range about 5 to 20 gmol/L was extended to higher densities, a maximum behavior occurred at about 25 gmol/L (Fig. 7). This maximum behavior agrees well with Haarhaus et al. [1995] who reported maximum solubility of 1,4-bis-(octadecylamino)-9,10-anthraquinone at density of about 22 gmol/L. But, the density at which maximum solubility occurs is slightly different from this study. This is because their dyes have different physical and chemical properties. Eq. (10) shows that the slope of the solubility isotherm in the plot of $\ln y_i$ versus $\ln\rho$ can be either positive or negative depending upon the value of the partial molar volume. It is positive at densities between 5 and 20 gmol/L. However, it becomes negative when the solubility goes over a maximum at higher densities. As the density of fluid decreases, we may have a minimum solubility at a small density. When the density goes below this value, the slope of solubility becomes negative again (not shown here).

3. Estimation of the Vapor Pressure

The vapor pressure or sublimation pressure is one of the requisites in analyzing the solid-fluid phase equilibrium. Even though the vapor pressure of a high molecular weight solute is too low to be measured experimentally, it can, at least, be estimated from the experimental solubility. The vapor pressures of the O30 disperse dye was estimated at four different temperatures from the solid-fluid equilibrium relationship (Eq. (3)). The fugacity coefficient of dye was obtained from Eqs. (5) and (12). The energy parameter $(a\alpha)_{AB}$ in Eq. (12) was correlated with the slope of the solubility isotherm (Eq. (11)) by using the experimental solubility data in pure CO_2 and the measured solid molar volume, which is taken as the size parameter, b_A. Using these vapor pressure data, we calculated the constants in the following vapor pressure equation:

$$\ln P_A^{vap} = A' + \frac{B'}{T} \tag{13}$$

The constants A' and B' for O30 were 16.66 and −6347, respectively. Fig. 8 shows near-linear relationship of the logarithm of the estimated vapor pressure (Table 2) versus inverse temperature, as expected for the usual solid materials. Thus we could confirm the validity of the vapor pressures obtained above for O30.

CONCLUSIONS

Solubility of C. I. Disperse Orange 30 dye in CO_2 increased with pressure and density at constant temperatures. The solubility versus density plot was much simpler than the solubility versus pressure plot. The isotherms were nearly straight and parallel to each other as seen in the previous studies. The empirical equations based on Chrastil's and Kumar and Johnston's equations fit the experimental solubility data fairly well, showing good consistency. We can predict solubility of O30 disperse dye at a temperature and a pressure using one of the two semi-empirical relationships.

The Peng-Robinson EOS was successfully used in correlating the dye solubility versus pressure or density. The size parameter in PR EOS was measured experimentally, while the energy parameter was obtained by correlation with experimental solubility data. With PR EOS we could predict the maximum solubility behavior that was caused by the difference in values of the solid molar volume and the partial molar volume. The vapor pressure obtained by correlating the solubility data with PR EOS also showed that our approach is acceptable.

ACKNOWLEDGMENTS

This research has been supported by the Yeungnam University Special Research Grant in 2003. It is partially supported by the research grant No. 96-E-ID02-19 from Korea Energy Management Corporation. We thank LG Chemical for the disperse dye samples.

REFERENCES

Baek, J.-K., "Solubility of Disperse Dyes in Supercritical Carbon Dioxide," M.S. Thesis, Yeungnam University (2001).

Bartle, K. D., Clifford, A. A. and Jafar, S. A., "Solubilities of Solids and Liquids of Low Volatility in Supercritical Carbon Dioxide," *J. Phys. Chem. Ref. Data*, **20**, 713 (1991).

Bartle, K. D., Clifford, A. A. and Shilstone, G. F., "Estimation of Solubilities in Supercritical Carbon Dioxide: A Correlation for the Peng-Robinson Interaction Parameters," *J. Supercrit. Fluids*, **5**, 220 (1992).

Chang, K.-H., Bae, H.-K. and Shim, J.-J., "Dyeing of PET Textile Fibers and Films in Supercritical Carbon Dioxide," *Korean J. Chem. Eng.*, **13**, 310 (1996).

Chrastil, J., "Solubility of Solids and Liquids in Supercritical Gases," *J. Phys. Chem.*, **86**, 3016 (1982).

Fat'hi, M. R., Yamini, Y., Sharghi, H. and Shamsipur, M., "Solubilities of Some 1,4-Dihydroxy-9,10-anthraquinone Derivatives in Supercritical Carbon Dioxide," *J. Chem. Eng. Data*, **43**, 400 (1998).

Haarhaus, U., Swidersky, P. and Schneider, G. M., "High-Pressure Investigations on the Solubility of Dispersion Dyestuffs in Supercritical Gases by VIS/NIR-Spectroscopy. Part I. 1,4-Bis-(octadecylamino)-9.10-anthraquinone and Disperse Orange in CO_2 and N_2O up to 180 MPa," *J. Supercrit. Fluids*, **8**, 100 (1995).

Kautz, C. B., Wagner, B. and Schneider, G. M., "High-Pressure Solubility of 1,4-bis-(n-alkylamino)-9,10-anthraquinones in Near- and Supercritical Carbon Dioxide," *J. Supercrit. Fluids*, **13**, 43 (1998).

Kumar, S. K. and Johnston, K. P., "Modeling the Solubility of Solids in Supercritical Fluids with Density as the Independent Variable," *J. Supercrit. Fluids*, **1**, 15 (1988).

Kurnik, R. T. and Reid, R. C., "Solubility Extrema in Solid-Fluid Equilibria," *AIChE J.*, **27**, 861 (1981).

Modell, M. and Reid, R. C., Thermodynamics and Its Applications, Prentice-Hall, Englewood Cliffs, N. J. (1983).

Muthukumaran, P., Gupta, R. B., Sung, H.-D., Shim, J.-J. and Bae, H.-K., "Dye Solubility in Supercritical Carbon Dioxide. Effect of Hydrogen Bonding with Cosolvents," *Korean J. Chem. Eng.*, **16**, 111 (1999).

Oezcan, A. S., Clifford, A. A., Bartle, K. D. and Lewis, D. M., "Solubility of Disperse Dyes in Supercritical Carbon Dioxide," *J. Chem. Eng. Data*, **42**, 590 (1997).

Peng, D.-Y. and Robinson, D. B., "A New Two-Constant Equation of State," *Ind. Eng. Chem., Fundam.*, **15**, 59 (1976).

Prausnitz, J. M., Lichtenthaler, R. N. and Azevedo, E. G. D., "Molecular Thermodynamics of Fluid-Phase Equilibria," Prentice-Hall, Upper Saddle River, New Jersey (1999).

Saus, W., Knittel, D. and Schollmeyer, E., "Dyeing of Textiles in Supercritical Carbon Dioxide," *Textile Res. J.*, **63**, 135 (1993).

Sung, H.-D., M. S. Thesis, Yeungnam University (1998).

Sung, H.-D. and Shim, J.-J., "Solubility of C. I. Disperse Red 60 and C. I. Disperse Blue 60 in Supercritical Carbon Dioxide," *J. Chem. Eng. Data*, **44**, 985 (1999).

Swidersky, P., Tuma, D. and Schneider, G. M., "High-Pressure Investigation on the Solubility of Anthraquinone Dyestuffs in Supercritical Gases by VIS-Spectroscopy. Part II," *J. Supercrit. Fluids*, **9**, 12 (1996).

Tuma, D. and Schneider, G. M., "High-Pressure Solubility of Disperse Dyes in Near- and Supercritical Fluids: Measurements up to 100 MPa by a Static Method," *J. Supercrit. Fluids*, **13**, 37 (1998).